

NIMROD analysis on MHD stability of negative triangularity tokamaks

Ping Zhu^{1,2}

on behalf of

S.-K. Cheng¹, R. Han¹, X.-T. Yan¹, and P. Zhu^{1,2} (USTC)
L.-J. Zheng³, M. T. Kotschenreuther³, and F. L. Waelbroeck³
(UT-IFS)

University of Science and Technology of China¹

University of Wisconsin-Madison²

University of Texas at Austin³

Center for Tokamak Transient Simulations Meeting

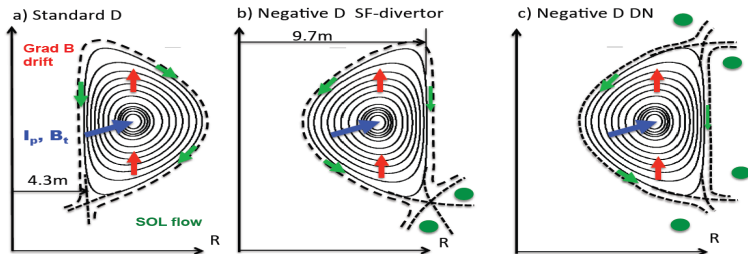
November 4, 2018

Portland, Oregon

Outline

- 1 Introduction and motivation
- 2 Simulation on DIII-D negative triangularity experiment
- 3 Comparison among different triangularity configurations in DIII-D type L-mode scenario
- 4 Simulation on advanced L-mode scenario with high bootstrap current fraction
- 5 Summary

Negative triangularity tokamak is beneficial for divertor design [M. Kikuchi et al, APFC (2014)]

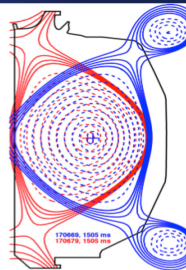
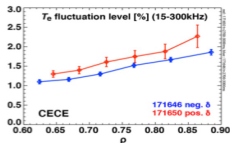
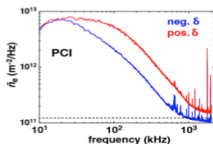


- Larger power handling area for the divertor $S_{div} \sim 2\pi R_{div}(F\Delta)$ ($R_{div}^{\delta < 0} > R_{div}^{\delta > 0}$). Δ is effective width of heat flux, F is the enhancement factor due to SF flux expansion.
- For example, heat flux can be 4 ~ 7 times smaller.
- Larger space for engineering design to mitigate the damage to divertor caused by particle and energy loads.

Turbulence and transport can be reduced in negative triangularity discharge compared to positive triangularity one [M. E. Austin et al, APS (2017)]

Summary: Negative Triangularity Discharges Created in DIII-D

- Unconventional **negative** triangularity ($-\delta$) discharges have been created in DIII-D
- Compared to matching **positive** δ , they have reduced turbulence and transport



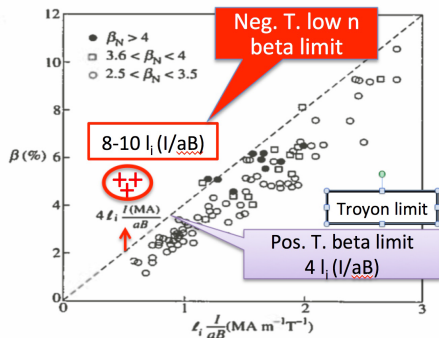
3

DIII-D
NATIONAL FUSION FACILITY

M.E. Austin/APS-DPP/2017-10-23

However, the β limit in negative triangularity plasma is often thought relatively low (e.g. $\beta_N \sim 2$) [S. Yu. Medvedev et al, Nucl. Fusion (2015)].

Recent ideal MHD stability study shows that negative triangularity L-mode with high bootstrap current fraction can achieve higher β than H-mode in positive triangularity case [L.-J. Zheng et al, Sherwood (2018)]



In this work, we use NIMROD to:

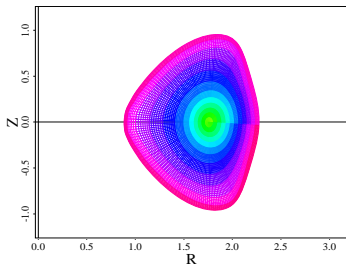
- Compare with previous ideal MHD stability study;
- Extend this study to non-ideal, nonlinear scenarios.

Outline

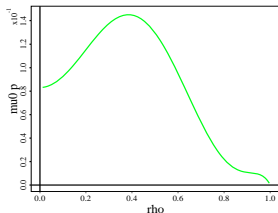
- 1 Introduction and motivation
- 2 Simulation on DIII-D negative triangularity experiment**
- 3 Comparison among different triangularity configurations in DIII-D type L-mode scenario
- 4 Simulation on advanced L-mode scenario with high bootstrap current fraction
- 5 Summary

DIII-D gfile g171421.03850 is used to generate simulation domain and equilibrium profiles

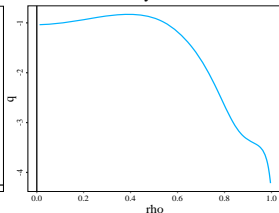
Finite Element Mesh



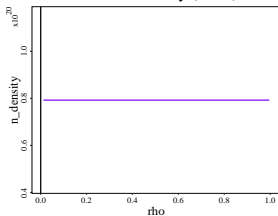
Plasma Pressure



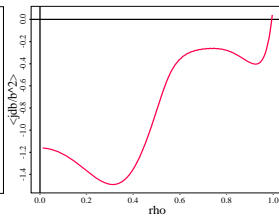
Safety Factor



Number Density (m^-3)



$\langle J.B/B^2 \rangle$



$n = 1$ linear growth rate scales as $\gamma \propto \eta^{0.49}$, contour plot shows (1, 1) mode structure (No vacuum region, ohms='mhd', uniform resistivity)

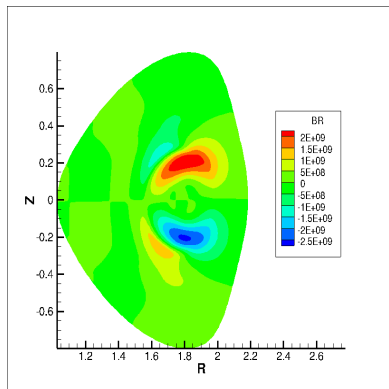
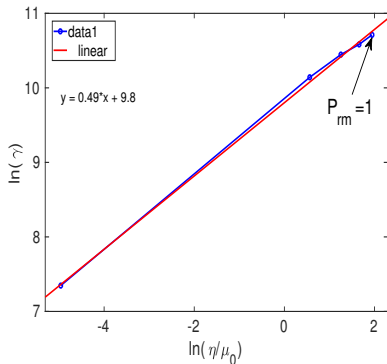
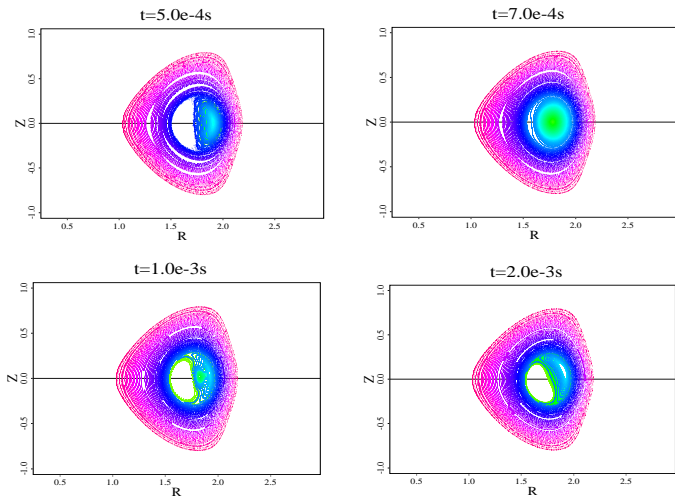
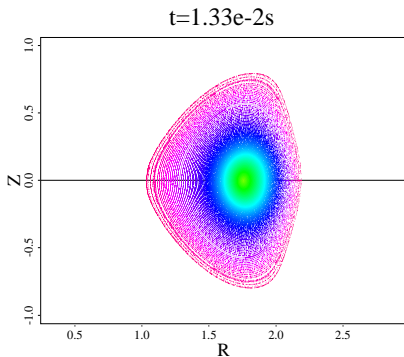
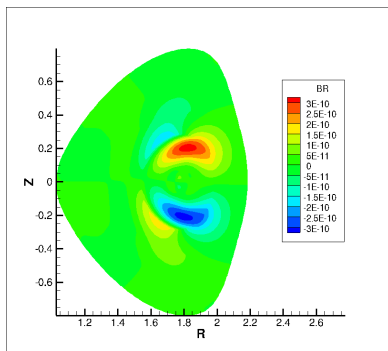


Figure: Viscosity is kept to be a constant so that $P_{rm} = 1$ at the point marked in the left plot.

When $S = 10^5$, poincare plots evolution shows the flux surface distortion and magnetic reconnection (nonlinear simulation, $n = 0 - 1$)

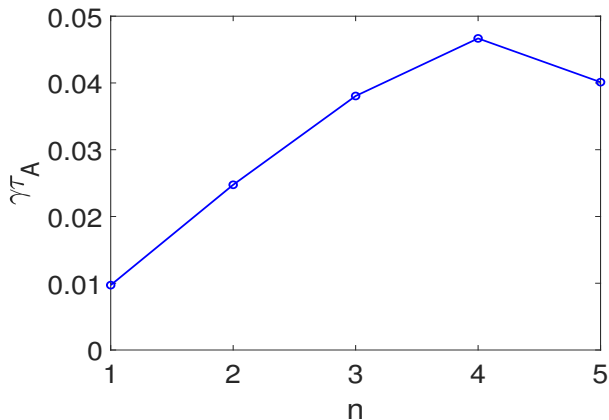


When $S = \infty$, $n = 1$ linear growth rate is nearly zero, no obvious flux surface distortion or reconnection is observed (nonlinear simulation, $n = 0 - 1$)



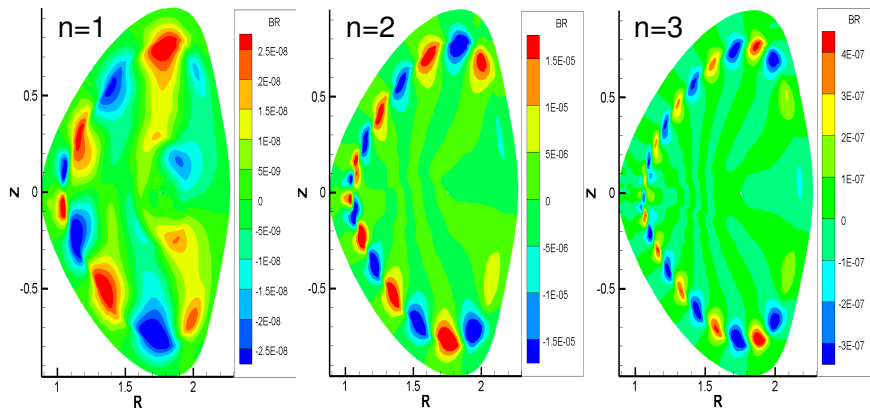
This negative triangularity configuration can be stable in ideal MHD limit.

We further include external mode in calculation (self-similar wall, ohms='2fl', Spitzer resistivity, high viscosity in vacuum region)



Linear growth rates typical of edge localized modes (ELMs).

Mode structure characteristic of ELMs



Two types of $n = 1$ mode structures have been found in the calculation

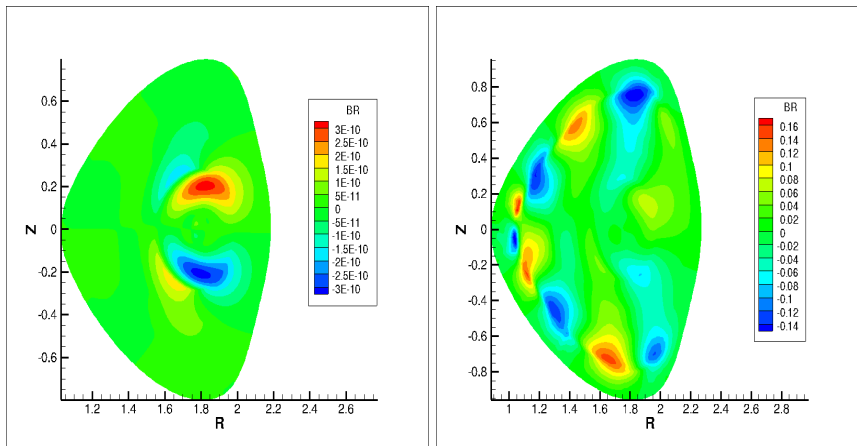


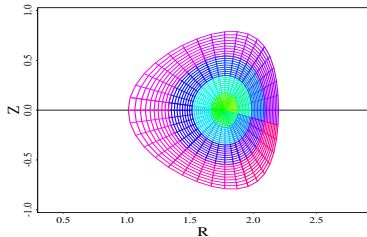
Figure: Left: No vacuum region, uniform resistivity; Right: Self-similar wall located at $b = 1.2$, Spitzer resistivity.

Outline

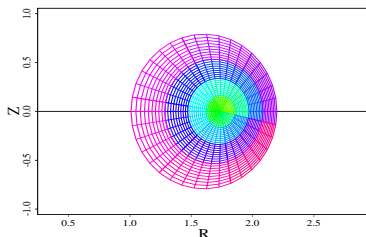
- 1 Introduction and motivation
- 2 Simulation on DIII-D negative triangularity experiment
- 3 Comparison among different triangularity configurations in DIII-D type L-mode scenario**
- 4 Simulation on advanced L-mode scenario with high bootstrap current fraction
- 5 Summary

Three kinds of triangularities based on DIII-D configuration adopted for comparison

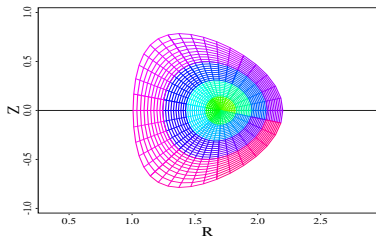
Finite Element Mesh



Finite Element Mesh

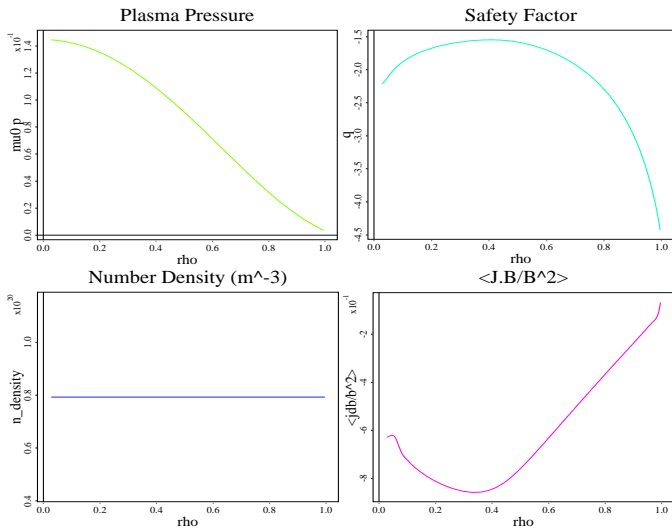


Finite Element Mesh

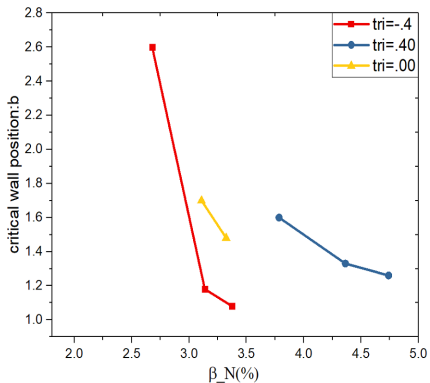


- Top left: $\delta = -0.4$
- Top right: $\delta = 0$
- Bottom left: $\delta = 0.4$

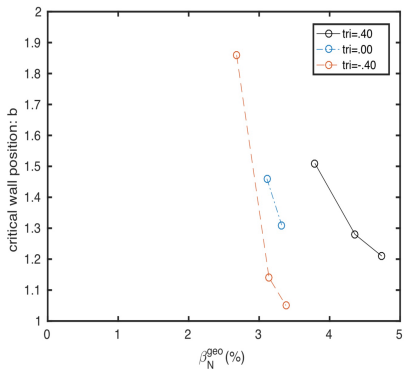
Equilibrium profiles used in analysis are DIII-D L-mode type



Critical wall positions for $n = 1$ mode from NIMROD consistent with AEGIS results



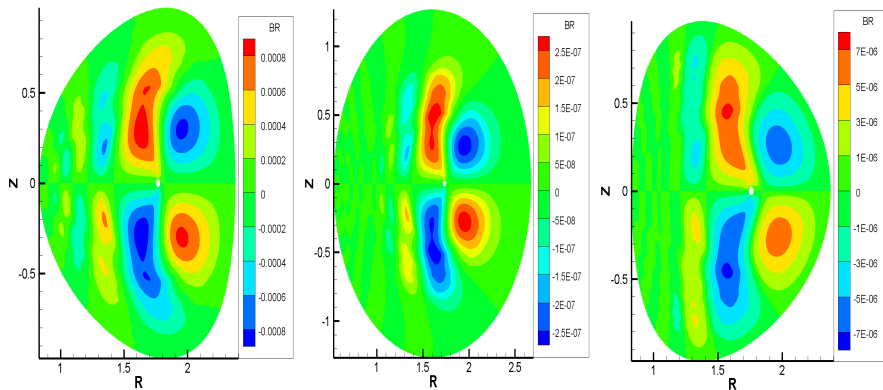
NIMROD simulation



AEGIS simulation [L.-J. Zheng et al, Sherwood (2018)]

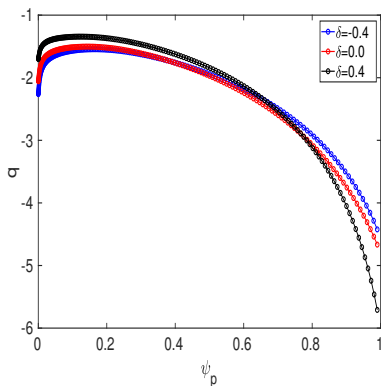
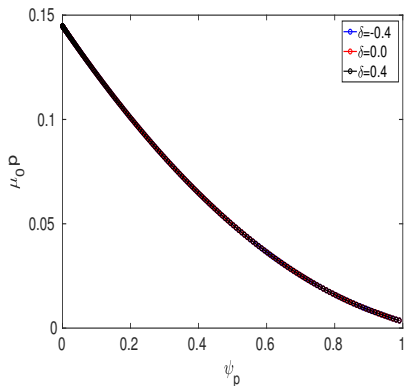
For a fixed wall position, β limit in negative triangularity configuration is lowest, but acceptable

(2, 1) mode structures are shown in three triangularity cases



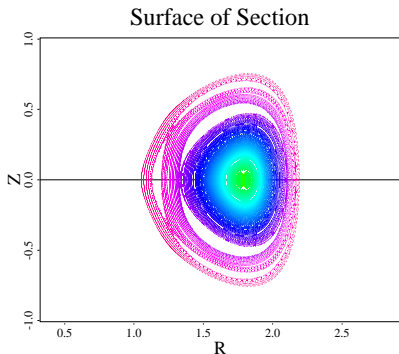
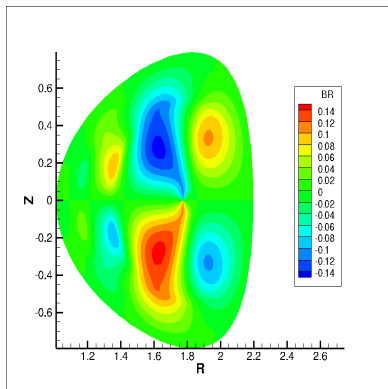
From left to right: $\delta = -0.4$, $\delta = 0$, $\delta = 0.4$

With similar equilibrium profiles, $n = 1$ internal mode stability is evaluated for three triangularities ($S = 10^5$, no vacuum region)



Left: pressure profiles; Right: safety factor profiles

(2, 1) unstable mode and magnetic island are found only in negative triangularity case. Positive and zero triangularity cases are stable

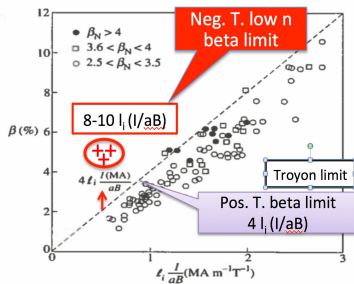
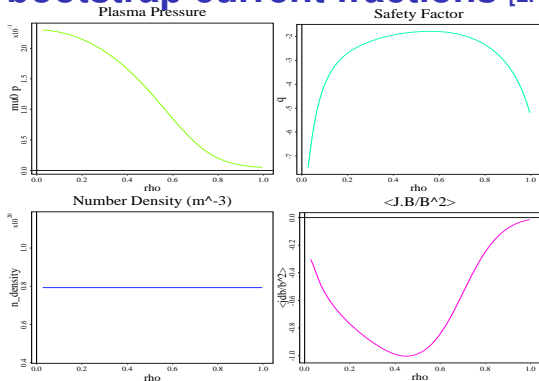


Negative triangularity more unstable for resistive internal mode as well.

Outline

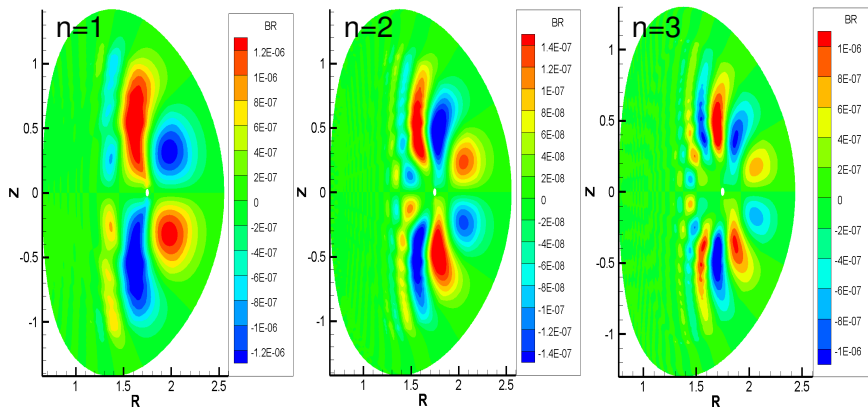
- 1 Introduction and motivation
- 2 Simulation on DIII-D negative triangularity experiment
- 3 Comparison among different triangularity configurations in DIII-D type L-mode scenario
- 4 Simulation on advanced L-mode scenario with high bootstrap current fraction**
- 5 Summary

Advanced scenarios of DIII-D L-mode profile can be obtained from reduced Ohmic and enhanced bootstrap current fractions [L.-J. Zheng et al, Sherwood (2018)]



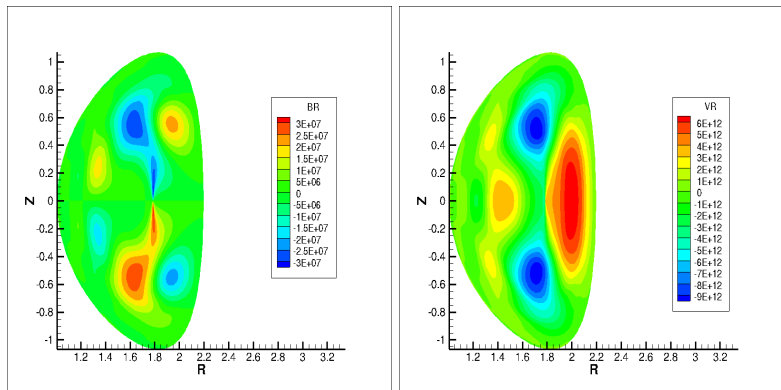
- Both AEGIS and DCON show that positive triangularity becomes unstable above Troyon limit.
- However low n kink modes remain stable in negative triangularity case when β is above Troyon limit.

NIMROD calculation on advanced scenario with positive triangularity is consistent with AEGIS results



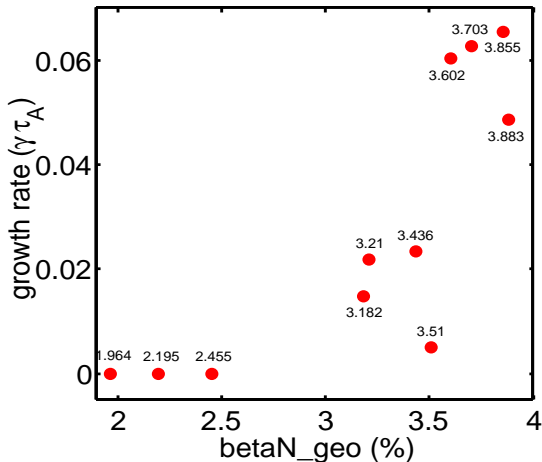
Comparison of critical wall positions (NIMROD/AEGIS):
 $1.43/1.4$ ($n=1$), $1.52/1.47$ ($n=2$), $1.28/1.4$ ($n=3$)

However, negative triangularity case is found $n = 1$ linearly unstable in NIMROD analysis (inconsistent with AEGIS/DCON)



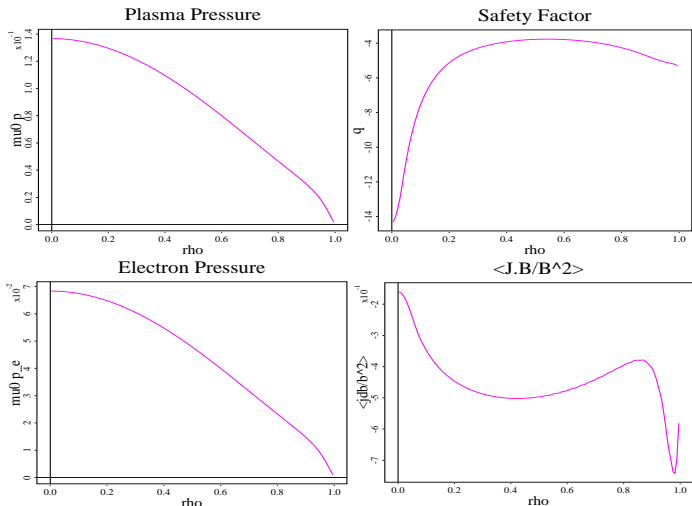
$n = 1$ linear growth rate seems independent on: η/μ_0 ($0 - 7m^2/s$);
viscous coefficient ($0 - 0.7m^2/s$); m_x/m_y ($36/36 - 144/144$).

Linear growth rate of $n = 1$ internal modes changes with β non-monotonically



One case looks special: $\beta = 3.51\%$.

Characteristics of this case: edge pedestal, strong reversed shear, bootstrap current near edge



This case may provide a possibility for profile optimization.

Outline

- 1 Introduction and motivation
- 2 Simulation on DIII-D negative triangularity experiment
- 3 Comparison among different triangularity configurations in DIII-D type L-mode scenario
- 4 Simulation on advanced L-mode scenario with high bootstrap current fraction
- 5 Summary

Summary

- NIMROD analysis on **DIII-D type L-mode** profiles for different triangularities:
 - ▶ Consistent $n = 1$ critical wall positions with AEGIS calculation;
 - ▶ For a fixed wall location, β limit in negative triangularity configuration is the lowest, but acceptable;
 - ▶ Comparison among different triangularities with similar equilibrium profiles shows negative triangularity the most unstable.
- NIMROD analysis on **advanced L-mode scenario (with high bootstrap current fraction)** profiles:
 - ▶ Consistent with AEGIS results in positive triangularity configuration;
 - ▶ But not in negative triangularity case (still under investigation);
 - ▶ There is a possibility for profile optimization.